

# The Selective Macroautophagic Degradation of Aggregated Proteins Requires the PI3P-Binding Protein Alf

Maria Filimonenko,<sup>1,8,9</sup> Pauline Isakson,<sup>1,8,9</sup> Kim D. Finley,<sup>2</sup> Monique Anderson,<sup>3</sup> Hyun Jeong,<sup>5</sup> Thomas J. Melia,<sup>6</sup> Bryan J. Bartlett,<sup>2</sup> Katherine M. Myers,<sup>3,4</sup> Hanne C.G. Birkeland,<sup>1</sup> Trond Lamark,<sup>7</sup> Dimitri Krainc,<sup>5</sup> Andreas Brech,<sup>1</sup> Harald Stenmark,<sup>1</sup> Anne Simonsen,<sup>1,9,\*</sup> and Ai Yamamoto<sup>3,4,\*</sup>

<sup>1</sup>Centre for Cancer Biomedicine, University of Oslo and Department of Biochemistry, The Norwegian Radium Hospital, Montebello, 0310 Oslo, Norway

<sup>2</sup>SDSU BioScience Center and Department of Biology, San Diego State University, San Diego, CA 92182, USA

<sup>3</sup>Department of Neurology

<sup>4</sup>Department of Pathology and Cell Biology

Columbia University, College of Physicians and Surgeons, 630 West 168th Street, New York, NY 10032, USA

<sup>5</sup>Department of Neurology, MIND, Harvard Medical School and Mass General Hospital, 114 16th Street, Charlestown, MA 02129, USA

<sup>6</sup>Department of Cell Biology, Yale University, New Haven, CT 06520, USA

<sup>7</sup>Biochemistry Department, Institute of Medical Biology, University of Tromsø, 9037 Tromsø, Norway

<sup>8</sup>These authors contributed equally to this work

<sup>9</sup>Present address: Department of Biochemistry, Institute of Basic Medical Sciences, University of Oslo, 0317 Oslo, Norway

\*Correspondence: [anne.simonsen@medisin.uio.no](mailto:anne.simonsen@medisin.uio.no) (A.S.), [ay46@columbia.edu](mailto:ay46@columbia.edu) (A.Y.)

DOI 10.1016/j.molcel.2010.04.007

## SUMMARY

There is growing evidence that macroautophagic cargo is not limited to bulk cytosol in response to starvation and can occur selectively for substrates, including aggregated proteins. It remains unclear, however, whether starvation-induced and selective macroautophagy share identical adaptor molecules to capture their cargo. Here, we report that Alf, a phosphatidylinositol 3-phosphate-binding protein, is central to the selective elimination of aggregated proteins. We report that the loss of Alf inhibits the clearance of inclusions, with little to no effect on the starvation response. Alf is recruited to intracellular inclusions and scaffolds a complex between p62(SQSTM1)-positive proteins and the autophagic effectors Atg5, Atg12, Atg16L, and LC3. Alf overexpression leads to elimination of aggregates in an Atg5-dependent manner and, likewise, to protection in a neuronal and *Drosophila* model of polyglutamine toxicity. We propose that Alf plays a key role in selective macroautophagy by bridging cargo to the molecular machinery that builds autophagosomes.

## INTRODUCTION

The fundamental ability of a cell to function is tightly linked to its capacity for protein synthesis. Equally important is the cell's ability to eliminate proteins that are deemed no longer necessary or misfolded. In light of this, it is unsurprising that a common cytopathological feature of disease is the presence of intracel-

lular inclusions. The pathological significance of aggregated proteins has been of particular interest in the area of neurodegeneration, as symptomatic reversal in mouse models of spinocerebellar ataxia 1 (SCA1) and Huntington's disease (HD) tightly correlates with the clearance of accumulated protein (Yamamoto et al., 2000; Zu et al., 2004).

Cytosolic proteins are degraded by the ubiquitin-proteasome and lysosome systems. In the last several years, the latter has been brought to the forefront with macroautophagy—a process through which cytosolic constituents are taken up into a multi-membranous structure known as the autophagosome, which upon fusion to endosomal (Berg et al., 1998; Filimonenko et al., 2007; Köchl et al., 2006) and lysosomal structures permits degradation (Klionsky, 2005). Predominantly known to nonspecifically engulf and degrade cytosol and long-lived proteins (LLP) in response to nutrient deprivation or inhibition of the kinase mTOR, macroautophagy also permits elimination of organelles such as mitochondria (Kanki et al., 2009; Klionsky, 2005; Okamoto et al., 2009). Recently, macroautophagy has been implicated in the elimination of aggregated proteins across various cell types, including neurons (Boland and Nixon, 2006; Iwata et al., 2005b; Ravikumar et al., 2002; Yamamoto et al., 2006). These proteins are often polyubiquitinated and can be recognized by the ubiquitin- and LC3-binding proteins p62 and NBR1 (Bjørkøy et al., 2005; Kirkin et al., 2009).

Alf (autophagy-linked FYVE protein, also known as WDFY3) is a 400 kDa protein that contains a BEACH domain, WD-40 domain, and a phosphatidylinositol 3-phosphate (PI3P)-binding FYVE domain (Simonsen et al., 2004). We have previously shown that it is recruited to ubiquitin-positive protein inclusions under stress conditions (Simonsen et al., 2004). Although mammalian studies of Alf have been limited, *Drosophila* lacking the Alf homolog Blue Cheese (*bchs*) are adult viable but have a reduced life span due to an accelerated accumulation

of ubiquitin-positive inclusions and neuronal degeneration (Finley et al., 2003). In this study, we demonstrate that aggregated proteins are sequestered into autophagic vesicles and present evidence that Alfy is essential for their macroautophagic clearance. Despite, however, its role in selective autophagy, Alfy is not required for macroautophagy due to nutrient deprivation. Alfy colocalizes and interacts with p62- and NBR1-positive proteins and directly interacts with Atg5. This interaction permits the creation of a greater complex with Atg12, Atg16L, and LC3, suggesting that Alfy acts as a scaffold that bridges its cargo to the macroautophagic machinery. Finally, we find that Alfy overexpression can decrease aggregated polyglutamine protein levels and protect cells from expanded polyglutamine toxicity in both a primary neuronal HD model and a *Drosophila* eye model of polyglutamine disease.

## RESULTS

### Polyglutamine Aggregates Can Be Found in Autophagosomes

Although macroautophagy has been implicated in several studies to eliminate aggregated proteins (Björkøy et al., 2005; Boland and Nixon, 2006; Iwata et al., 2005b; Kirkin et al., 2009; Ravikumar et al., 2002; Yamamoto et al., 2006), it is uncertain whether oligomers or larger protein aggregates and inclusions are trafficked to autophagosomes. To examine this issue further, we turned to a model aggregation-prone protein, a short fragment of the protein huntingtin (exon1Htt) that carries an expanded polyglutamine (polyQ) mutation of greater than 37 glutamines (37Q). These proteins spontaneously aggregate in vitro and are found as aggregated oligomers to large, aggregate-like inclusions in vivo. This is readily observed with transient transfection of a Flag-tagged exon1Htt construct expressing 68 polyQ (Flag-HttQ68, HeLa) (Figure S1A available online), as well as in previously described tetracycline (tet)-regulatable cell lines (HeLa and N2a) stably expressing the first 17 amino acids of Htt followed by a polyQ expansion (65Q or 103Q) tagged to monomeric CFP (HttPolyQ-mCFP) (Figure 1) (Yamamoto et al., 2006). As a control, we used cell lines that express 25Q, which is under the aggregation threshold of 37 repeats and thus remains soluble (Yamamoto et al., 2006).

We previously reported that polyQ aggregates and inclusions can colocalize to transiently transfected LC3-YFP (Yamamoto et al., 2006). Transient expression of Flag-HttQ68 in cell lines stably expressing LC3-GFP leads to similar results (Figure S1A). To ensure that the colocalization of LC3 to inclusions is indeed indicative of the presence of autophagic membrane, we next used ultrastructural and biochemical approaches (Figures 1A–1G). Lysosomal inhibitors increased the frequency with which LC3 colocalized to the mCFP-positive inclusion (Yamamoto et al., 2006), possibly by inhibiting the maturation of autophagosomes to autolysosomes. Htt103Q- and 65Q-mCFP stable cell lines were thus pretreated with Bafilomycin A1 (BafA1) and then processed for ultrastructural analyses. As expected, inclusions of differing sizes were detected by electron microscopy (EM). The majority of inclusions, especially larger inclusions of several microns in diameter, were found membrane free (Figures 1A and S1B). In contrast, smaller polyQ inclusions

up to 1  $\mu$ m in diameter were preferentially detected within double-membrane structures (Figures 1B, S1D, and S1E). In rare cases, we could observe larger aggregates (up to 5  $\mu$ m diameter) surrounded by a double-membrane structure (Figure S1, double arrow in inset in C). Quantification of inclusions based on size (less than [ $<$ ] or greater than [ $>$ ] 1  $\mu$ m) and localization (cytosolic [cyto] or sequestered [seq]) is shown in Figure 1C.

To independently determine whether inclusions are found in autophagic vesicles (AV), we next performed cell fractionation experiments with nycodenz (Strømhaug et al., 1998) (Figure 1Da) or metrizamide (Marzella et al., 1982) (Figure 1Db) to isolate the AV fractions from Htt103Q-mCFP cells. These experiments were performed in the absence of lysosomal inhibitors. Cryo EM analysis revealed that multilamellar vesicles can be clearly detected in the AV fraction (Figure 1E). Moreover, the AV fraction was enriched for membrane-bound LC3 (form II), confirming autophagosome enrichment (Figure 1F), whereas cytosolic fractions were positive for only soluble LC3 (form I). To determine whether SDS-insoluble aggregates can be found in the AV fraction, we probed for Htt103Q-mCFP using an antibody against mCFP. In those fractions enriched for LC3- II, Htt103Q-mCFP remains in the stacking gel, indicative of the presence of SDS-insoluble aggregated Htt (Figure 1G) (Cornett et al., 2005). The same fractions were also associated with a high-molecular weight polyubiquitin smear (Figure S1F and S1G) (Davies et al., 1997; DiFiglia et al., 1997). Taken together, these data indicate that SDS-insoluble aggregates can be found sequestered in double-membrane structures and in an AV-enriched fraction.

### Alfy Shuttles from the Nuclear Membrane to Colocalize with Aggregated Proteins

We have previously reported that Alfy is a predominantly nuclear protein that is recruited to cytoplasmic ubiquitinated structures in response to cellular stress such as proteasome inhibition (Simonsen et al., 2004). We therefore examined whether expression of aggregated polyQ proteins also recruited Alfy. Immunofluorescence (IF) revealed that, in the absence of aggregated proteins, Alfy is largely found within the nucleus along the nuclear membrane, colocalizing with nucleoporins (Figure 2A). The presence of the cytosolic polyQ inclusions led to the presence of Alfy in the cytosol, colocalized to the inclusions (Figure 2B). To determine whether Alfy shuttled from the nucleus, cells were treated with leptomycin B (LMB), an inhibitor of nuclear export, and were re-examined. Treatment with LMB significantly diminished the localization of Alfy to the inclusions, indicating that Alfy is actively exported from the nucleus in a CRM1-dependent manner (Figures 2C and 2D). LMB treatment also inhibited the recruitment of Alfy to cytoplasmic ubiquitin-positive aggregates due to starvation-induced stress (Figure 2E). qRT-PCR analysis also showed that Alfy mRNA levels were unaffected by polyQ aggregation, indicating that de novo synthesis of Alfy in response to aggregation is unlikely (Figure 2F). Of interest, inhibition of nuclear export caused increased colocalization of Alfy with promyelocytic leukemia (PML) nuclear bodies (Figures S2A and S2B), intranuclear sites where misfolded proteins have been proposed to accumulate (Rockel et al., 2005). Consistent with this, Alfy colocalized with intranuclear inclusions of the nuclear protein Ataxin-1 (Figures S2C

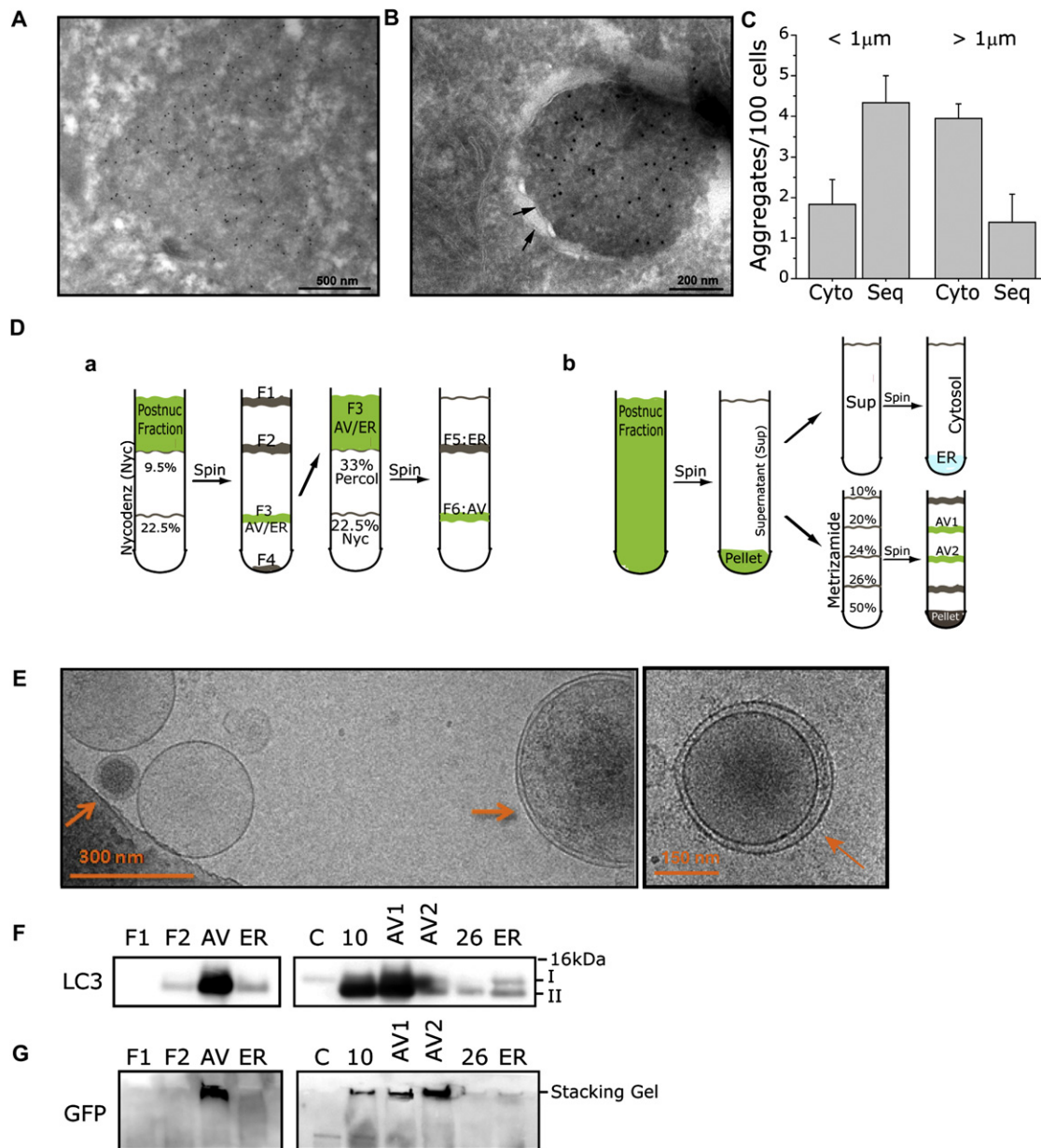


**Figure 1. Polyglutamine Aggregates Are Found in Autophagic Vacuoles**

(A–G) Polyglutamine aggregates can be found in double-membrane structures by immuno-EM and in the autophagosome fraction of cell fractionation experiments.

(A–C) Immuno-EM analysis of Htt103Q-mCFP cell lines. Cells were treated for 4 hr with BafA1 and then fixed. Gold particles label structures positive for mCFP.

(A) Membrane-free aggregates.

(B) Aggregates sequestered within a double membrane.

(C) Quantification of cytosolic (Cyto) versus sequestered (Seq) aggregates. Aggregates positive for GFP were sorted based on diameter (< or > 1 μm) and then counted. Less than 1 μm aggregates were more likely to be sequestered in autophagosomes (Cyto: 2.11 ± 0.408; Seq: 4.10 ± 0.689), whereas greater than 1 μm aggregates were cytosolic (Cyto: 3.94 ± 0.372; Seq: 1.40 ± 0.700). 185 cells were counted across n = 3 experiments. Data are shown as mean ± SEM.

(D–G) Cell fractionation experiments using two distinct protocols reveal that SDS-insoluble Htt103Q-mCFP-positive proteins can be found in the autophagosome (AV) fractions.

(D) Summary of fractionation protocols used.

(E) Cryo EM images generated from AV fractions using Nycodenz protocol.

(F) Immunoblot analysis of cellular fractions. LC3 II is enriched in AV fractions.

(G) Immunoblotting of AV fractions reveals the presence of SDS-insoluble Htt103Q-mCFP in the loading stack of the gel, despite using denaturing conditions. 4%–12% polyacrylamide gels were used for SDS-PAGE.

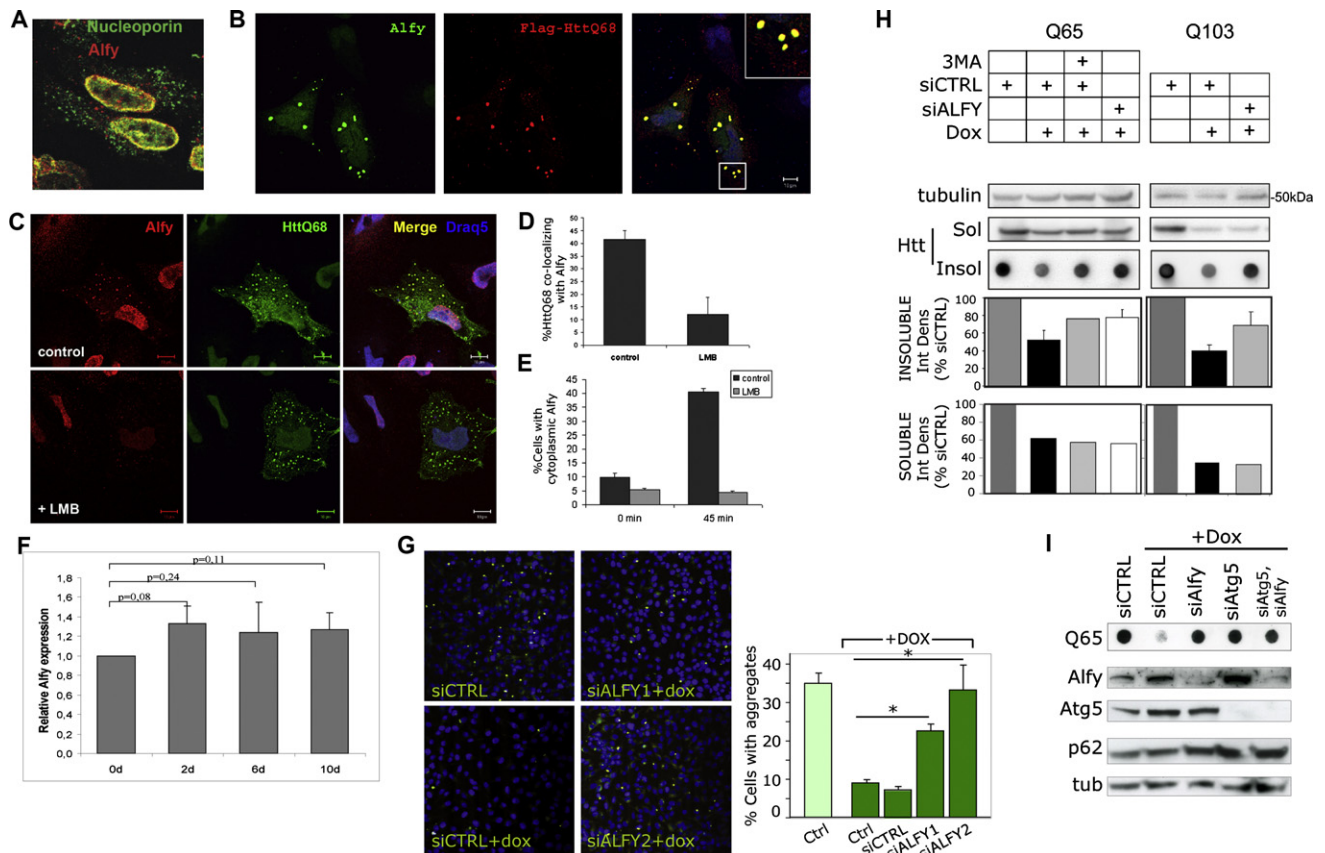


**Figure 2. Alfy Translocates from the Nucleus and Is Required to Clear Aggregated PolyQ**

(A–F) Alfy translocates from the nucleus into cytoplasmic structures.

(A) Alfy localizes to the nuclear membrane in untreated HeLa cells and colocalizes with nucleoporin.

(B) HeLa cells were transfected with Flag-HttQ68 (red) and probed for endogenous Alfy (green). Inset shows colocalization of Alfy and the polyQ inclusions (yellow).

(C and D) Flag-HttQ68 (green) transfected cells were treated 40 hr later with 5 nM leptomycin B for 4 hr, fixed, and stained with anti-Alfy antibodies (red). Draq5 (blue) labels nuclei. Scale bar = 10  $\mu$ m. LMB treatment inhibited recruitment of Alfy to cytoplasmic inclusions (30 cells, two independent experiments). Student's *t* test;  $p < 0.005$ .

(E) LMB inhibits Alfy translocation under nutrient-rich and nutrient-starved conditions. HeLa cells were starved for 45 min in HBSS  $\pm$  LMB. Cells containing cytoplasmic Alfy-positive structures were counted ( $n > 300$  cells from  $n = 3$  experiments).

(F) Htt103Q-mCFP cells were treated with dox to abolish expression (7 days). Dox was then removed to re-establish expression. Cells were collected at days 0, 2, 6, and 10. Relative Alfy mRNA levels were determined by qRT-PCR and normalized to day 0. TBP and actin were used as controls. Two experiments were performed in duplicate.

(G–I) Alfy is required for clearance of expanded polyQ aggregates.

(G) Htt103Q-mCFP cells were quantified for mCFP puncta per cell. 100  $\mu$ g/ml dox for 5 days led to a significant decrease of percentage of cells with aggregates ( $p < 0.001$ ). siALFY1 and siALFY2 significantly inhibited clearance ( $p < 0.001$ ), whereas siCTRL did not ( $p = 0.3218$ ). Representative confocal images of each group generated on the INCA3000 are shown. Nuclei are stained with Hoechst33342 (blue), and HttQ103-mCFP puncta are in green.

(H and I) Htt65Q- and Htt103Q-mCFP were transfected with siCTRL or siALFY and exposed 48 hr later to dox for 3 days.

(H) Alfy KD inhibited clearance of SDS-insoluble protein for 65Q ( $p < 0.05$ ) and 103Q ( $p < 0.05$ ) cells (Student's *t* test). No detectable change was seen in SDS-soluble proteins as shown by SDS-PAGE. Macroautophagy control was 5 mM 3MA for 48 hr.

(I) Alfy KD and Atg5 KD inhibited clearance of SDS-insoluble inclusions.

All data are shown as mean  $\pm$  SD. Complete statistics can be found in [Supplemental Experimental Procedures](#) under "Statistical Information for Figures."

and S2D). Colocalization with other intranuclear structures was not detected (Figure S2B).

### Alfy Is Required for Macroautophagy-Mediated Clearance of Aggregated Protein

But why is Alfy recruited to these aggregating proteins? In previous studies, we and others have shown that macroautoph-

agy is required to clear protein aggregates (Iwata et al., 2005a, 2005b; Ravikumar et al., 2002; Yamamoto et al., 2006). To analyze aggregate clearance, HttPolyQ-mCFP cell lines were treated with doxycycline (dox) (Yamamoto et al., 2006), which led to inclusion clearance over several days in a macroautophagy-dependent manner (Figures S2 and S3) (Yamamoto et al., 2006) (quantified as the number of mCFP puncta per cell). To



determine whether Alfy plays a role in clearance, we transfected siRNA sequences against Alfy (siALFY), which significantly impeded clearance of aggregated polyQ protein (Figure 2G). A control sequence (siCTRL) had no effect.

To independently quantify the impact of Alfy knockdown (KD) on aggregate clearance, we used a filter trap assay, which has been successfully used by several groups to examine the presence of SDS-insoluble aggregates (Bailey et al., 2002; Passani et al., 2000; Wanker et al., 1999). Alfy KD significantly inhibited clearance of insoluble Htt65Q- or Htt103Q-mCFP (Figure 2H, dot blots). The degree of inhibition due to Alfy KD was comparable to the effect of 3-methyladenine (3MA), a chemical inhibitor of macroautophagy. Similar Alfy dependence was obtained in N2a Htt103Q-mCFP cells (Figure S3D). Codepletion of Alfy and Atg5 led to no detectable further inhibition of Htt polyQ clearance, compared to depletion of each protein individually (Figures 2I and S3D), suggesting that Alfy eliminated the aggregated polyQ proteins by macroautophagy. Moreover, Alfy KD had no measurable effect on the chymotrypsin-like activity of the proteasome, suggesting that Alfy is not required for proteasome activity (Figure S3E). Of interest, western blot analysis of the SDS-soluble Htt65Q- or 103Q-mCFP protein indicated that Alfy KD had little effect on the decrease of soluble polyQ protein (Figure 2H); however, because it is unclear whether this decrease is due to degradation of the SDS-soluble protein or conversion to an SDS-insoluble pool, we examined the clearance of nonaggregating Htt25Q-mCFP. Although 3MA and BafA1 treatment somewhat inhibited clearance of Htt25Q-mCFP, Alfy KD had no effect (Figures S2F and S2G), indicating that Alfy is not involved in lysosomal clearance of nonaggregated polyQ proteins.

### Alfy Is Not Required for Starvation-Induced Macroautophagy

The requirement of Alfy for macroautophagic clearance of aggregated proteins implies that it may be required for general starvation-induced macroautophagy. We therefore determined the Alfy dependence of macroautophagy in response to amino acid withdrawal (Klionsky et al., 2008) (Figure 3). We first examined the degradation of LLPs in both HeLa and N2a cells subjected to serum and amino acid withdrawal. As expected, a significant increase in LLP proteolysis that was 3MA dependent was observed in both cell types (Figure 3A, Starv+3MA). Although KD of Beclin1 also inhibited LLP degradation (Figure S2C), depletion of Alfy had no significant effect (Figure 3A). Constitutive gene knockdown in cell lines stably expressing shRNA against Alfy also showed no deficits in LLP degradation (Figure S2H).

We next explored whether Alfy is required for LC3 lipidation. The conversion of cytosolic LC3 (form I) to membrane-bound LC3 (form II) has been correlated with autophagosome production (Kabeya et al., 2000). Neither starvation-induced (Figure 3B) nor basal lipidation (Figure 3C) was affected by Alfy depletion. In a complementary experiment, we examined endogenous LC3 puncta formation in response to starvation. CTRL cells, ALFY-depleted cells, and Atg7-depleted (siAtg7) cells were starved for 4 hr in the presence of BafA1 and were stained for endogenous LC3 (Iwata et al., 2005b) (Figure 3D). Starvation led to a significant increase of LC3 puncta in control cells, which

was inhibited in the absence of Atg7. In contrast, Alfy KD had no significant impact on LC3 puncta formation, consistent with the LC3 conversion data (Figure 3B). Finally, EM analyses of cells after starvation also showed no observable difference in autophagosome formation after Alfy KD (Figure 3E).

To further clarify the role of Alfy in starvation under physiologic conditions, we examined the role of its *Drosophila* homolog *bchs* in the starvation response of the larval fat body. Previous studies have shown that rapid onset of starvation-induced autophagy can be reliably followed in fat body cells by following autolysosomal content using the marker Lysotracker Red (LR) or a fluorescent autophagy marker, GFP-Atg8a (Lindmo et al., 2006; Rusten et al., 2004; Scott et al., 2004). Fat body tissue isolated from wild-type (WT), two different *bchs* mutants (*bchs*<sup>3</sup> and *bchs*<sup>7</sup>) (Finley et al., 2003), and Atg1-depleted (*CG-GAL4;UAS-dsAtg1-RNAi*) fed or starved second instar larvae were incubated with LR, and autolysosome accumulation was examined (Figures 3F and S4). Fat bodies dissected from fed larvae of all genotypes showed diffuse staining, with little to no detectable punctate structures. In contrast, starvation for 3 hr caused wild-type and *bchs* mutant larvae to display intense, punctate LR staining in fat body cells (Figures 3F, *bchs*<sup>3</sup>, and S4A, *bchs*<sup>7</sup>). Larvae expressing *dsAtg1-RNAi* in the fat body had significantly fewer puncta, indicating that starvation-induced autophagy can be inhibited at this developmental stage. Similar patterns were also detected using LR in combination with a GFP-Atg8a (Figure S4B). These data provide further evidence that Alfy/Bchs is not an essential component for a response to cellular starvation.

### Alfy Directly Interacts with Atg5 and Can Be Found in a Complex with Atg5, Atg12, and Atg16L

We next sought to determine how Alfy contributes to the degradation of aggregation-prone proteins. The C terminus of Alfy contains protein-protein interaction domains, such as a Beige and Chediak-Higashi (BEACH) domain and WD-40 repeats, and a PI3P-binding FYVE domain (Figure 4A). In light of the potential of Alfy to interact with both protein and lipid, we hypothesized that Alfy may act as a scaffold for the macroautophagic machinery onto the aggregation-prone protein.

Using IF, we found that endogenous Alfy colocalizes with endogenous Atg5 (Figure 4A, panel i), and they both localize to the polyQ inclusion in the stable Htt103Q-mCFP cells (Figure S5A). To determine which region of Alfy is required for the colocalization with endogenous Atg5, different regions of Alfy tagged to the fluorophore tdTomato were overexpressed in non-starved cells. We found that the Atg5-Alfy colocalization required the C-terminal region of Alfy encoding the WD40 repeats (Figure 4A, panels ii, iv, and vi), whereas the BEACH domain (Figure 4A, panel iii) and FYVE domain (Figure 4A, panel v) were not required. There was no colocalization of the N-terminal portion of Alfy with Atg5 (Figure S5B).

To further resolve the nature of this colocalization, we next performed coimmunoprecipitation (co-IP) experiments using overexpressed and recombinant deletion mutants of Alfy. As shown in Figure 4B, overexpression of myc-tagged Atg5 coimmunoprecipitated with the same fragment of tdTomato-tagged Alfy that colocalized in Figure 4A, panel iv (Alfy<sub>2981–3526</sub>). In contrast, overexpression of the myc tag alone did not co-IP

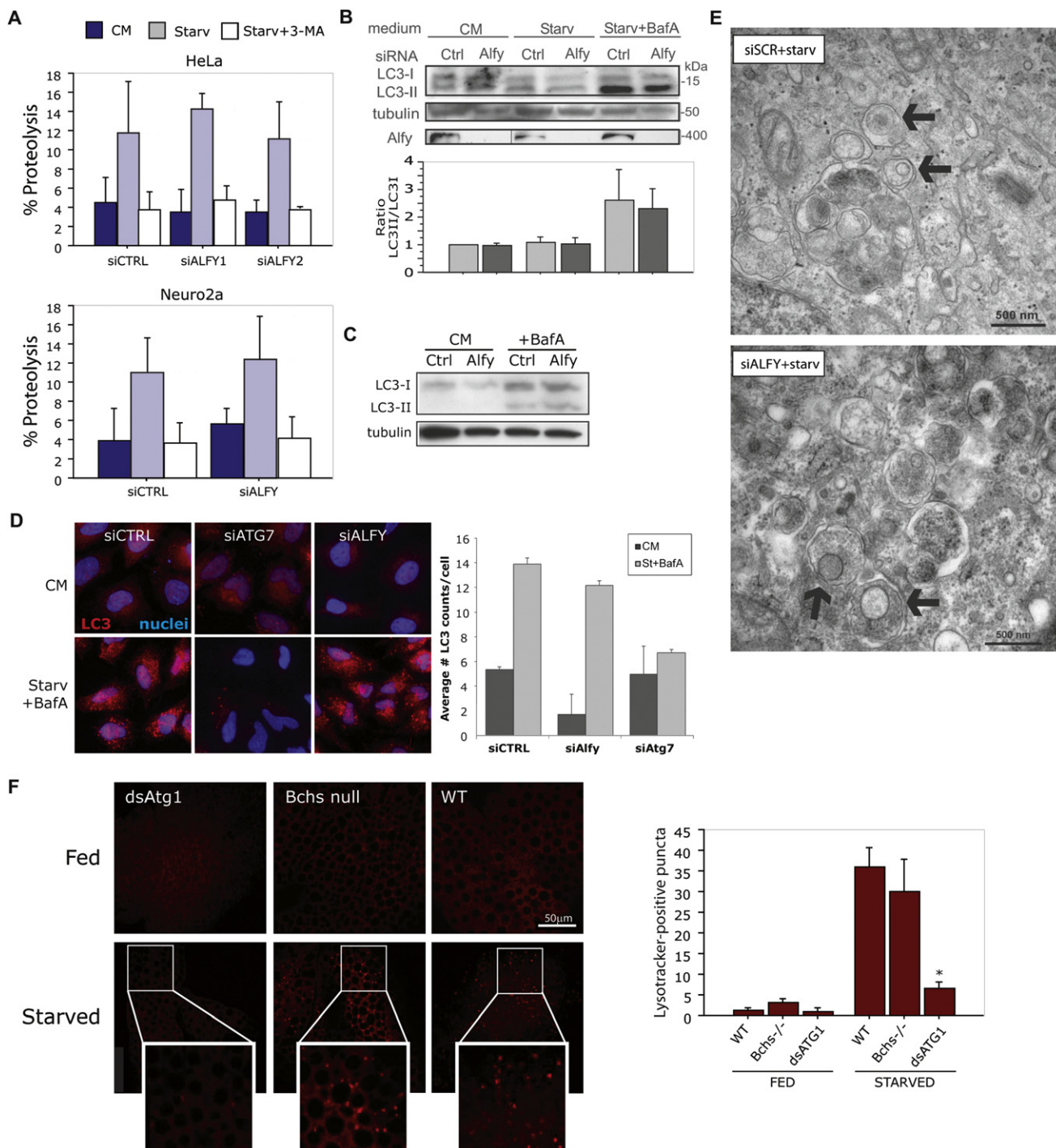


**Figure 3. Alfy Is Not Required for Starvation-Induced Autophagy**

(A) Alfy is not required for LLP degradation. Amino acid withdrawal (Starv) leads to a significant effect in both HeLa and N2a cells. Knockdown of Alfy had no significant effect on LLP degradation (HeLa,  $p = 0.6991$ ; N2a,  $p = 0.3505$ ). To ensure that LLP degradation was due to macroautophagy, starvation experiments were also performed + 10 mM 3MA. Cells were transfected with siCTRL or siALFY and then monitored for LLP degradation 72 hr later ( $n = 3$  experiments in duplicate or triplicate).

(B and C) Alfy depletion has no effect on starvation-induced or basal (C) LC3 lipidation ( $p = 0.7641$ ;  $n = 4$ ). HeLa cells transfected with siALFY or siCTRL were cultured in complete medium (CM) or starved (Starv) in the absence or presence of BafA1 for 4 hr (B) or 2 hr (C).

(D) Alfy depletion has no effect on LC3 puncta formation. Cells transfected with siCTRL, siATG7, or siALFY were starved, fixed, and stained for endogenous LC3. In starved cells, there is a significantly greater number of LC3-positive puncta in siCTRL and siALFY cells, whereas siATG7 cells have significantly fewer LC3-positive puncta upon starvation between siCTRL and siATG7 ( $p < 0.0001$ ) and siALFY and siATG7 ( $p < 0.0001$ ). Error bars represent mean + SD ( $n = 8$ ).

Alfy. To determine whether this interaction was direct, recombinant GST-tagged Atg5 was incubated with the C-terminal WD40-containing region of Alfy fused to maltose-binding protein (MBP-Alfy<sub>2888–3526</sub>). MBP-Alfy<sub>2888–3526</sub> was pulled down with GST-Atg5, indicating that this region of Alfy interacts directly with Atg5. To ensure the specificity of this interaction, GST-LC3 and GST-Syntaxin-7 were used as negative controls (Figure 4C). Next, yeast two-hybrid (Y2H) confirmed a positive interaction between the WD40 repeats of Alfy and Atg5 in both a  $\beta$ -galactosidase liquid assay and a growth selection assay scoring for the *HIS3* reporter (Figure 4D, S5C). No growth was detected with the FYVE domain alone or a control (Figure 4D). These results are consistent with the data from our co-localization studies and strongly indicate that Alfy directly interacts with Atg5 through the WD-40 domain. Because overexpression can yield false-positive results, we also examined whether this interaction can be found with endogenous proteins (Figure 4E). Whole-cell lysates from immortalized WT and ATG5KO mouse embryonic fibroblasts (MEFs) (Hosokawa et al., 2006) were incubated with anti-Alfy or Ctrl serum and were immunoprecipitated using protein A beads. Atg5 can be found in a complex with endogenous Alfy in WT cells, confirming that Alfy and Atg5 interact. No precipitation was observed in either Atg5KO MEFs or serum control IP in WT MEFs.

Though the monomeric form of Atg5 is ~35 kDa, the co-IP experiment revealed an ~56 kDa protein. This higher-molecular weight species is indicative of the Atg5-Atg12 complex, which is the predominant form at which Atg5 is found in vivo. Indeed, probing for Atg12 confirmed the presence of the Atg5-Atg12 complex because Atg12 was also found at 56 kDa (Figure 4F). Moreover, probing for Atg16L also revealed its presence (Figure 4F), strongly suggesting that, in cells, Alfy can be found in a complex with the Atg5-Atg12-Atg16L E3-like ligase for the lipidation of LC3 (Fujita et al., 2008).

### Alfy Scaffolds the Aggregation-Prone Protein with the Macroautophagic Machinery

We have thus far determined that Alfy is required for macroautophagy-mediated clearance of aggregated polyQ protein and that it can form a complex with Atg5-Atg12-Atg16L. We next asked whether Alfy forms a complex with aggregated polyQ to potentially recruit the autophagic machinery to the inclusions. IF showed that endogenous, full-length Alfy colocalized with the Htt inclusions (Figure 2B). To determine whether this is indicative that Alfy and aggregated mutant Htt is in a complex, we performed co-IP experiments. The polyQ protein tag was immunoprecipitated by its fluorophore from lysates generated from either the HttpolyQ-mCFP stable cell lines or a primary neuronal lentiviral model that expresses an exon1 fragment of Htt with

72Q (exon1Htt72Q) tagged to GFP (Figure 5A). Alfy coimmunoprecipitated with Htt65Q- and 103Q-mCFP, as well as with exon1Htt72Q. Of interest, Alfy did not co-IP with Htt25Q-mCFP (Figure 5A), consistent with our findings that Alfy is not required for the elimination of soluble polyQ proteins (Figures 2H and S3).

To delineate which portion of Alfy may interact with the aggregating protein, an N-terminal fragment (Alfy<sub>1–1271</sub>), a central fragment (Alfy<sub>2285–2981</sub>), and a C-terminal fragment (Alfy<sub>2981–3526</sub>) tagged to tdTomato were overexpressed in Htt103Q-mCFP cells. Two different patterns emerged (Figure S6A). The N-terminal fragment completely colocalized with the Htt aggregate, suggesting that it was distributed throughout or decorated the outside of the inclusion. In contrast, the C-terminal fragment was only found to decorate the outside of the inclusion. The internal Alfy fragment or tdTomato alone neither colocalized with nor coated the inclusion (Figure S6A). To determine whether the colocalization indicated that the proteins were in a complex, we performed co-IP experiments (Figure 5B). A myc-tagged Alfy<sub>1–1271</sub> was found to complex with Htt103Q-mCFP. Under the same stringency conditions, the myc-tagged Alfy<sub>2981–3526</sub> was also bound to Htt103Q-mCFP. Taken together, both the N- and C-terminal fragments of Alfy can interact with the polyQ protein.

We next sought to determine whether Alfy can recruit Atg5 or any other autophagic proteins to the polyQ protein aggregates (Figure 5A). Further immunoblotting revealed that endogenous Atg5, LC3 (forms I and II), and p62 also co-IP with the aggregated HttpolyQ protein, both in the stable cell lines and in the neuronal lentiviral model (Figure 5A). The interaction appeared specific because another macroautophagic protein, Atg7, failed to co-IP with the mutant polyQ protein (Figures 5C and 5D). Moreover, whereas Alfy was required for recruitment of Atg5 to the inclusion, interaction of Alfy with the polyQ protein did not require the presence of Atg5 (Figure S6B). Finally, consistent with Alfy recruitment, Atg5 did not co-IP with Htt25Q-mCFP. LC3 (forms I and II) and p62 were also absent (Figure 5A).

To further ascertain whether Alfy is central to recruiting Atg5 to the aggregates, we used RNAi to deplete Alfy in Htt103Q-mCFP cells (Figure 5D) and in neurons (Figure 5E) and re-examined the complex. Decreased Alfy levels diminished the interaction with Atg5 to a degree consistent with KD efficiency. The interaction of p62 with Htt103QmCFP, however, was not Alfy dependent, consistent with p62 interacting with polyQ proteins in a ubiquitin-dependent manner (Bjørkøy et al., 2005). Unexpectedly, Alfy KD led to a diminished amount of LC3 present in the complex (Figures 5D and 5E). Because there was no direct interaction of C terminus Alfy with LC3 (Figure 4C), this data implies that Alfy-mediated recruitment of Atg5 to the inclusion might

(E) EM reveals no detectable difference in autophagosome (black arrows) formation due to Alfy depletion. siALFY- or siCTRL-transfected cells were starved for 4 hr before fixation and imaging.

(F) Autolysosome accumulation in *Drosophila* fat body cells is not dependent on Bchs. In response to starvation (3 hr sucrose;  $n = 3$ ), WT larvae ( $n = 3$ ) show an increase in autolysosome numbers, whereas loss of Bchs (*bchs<sup>3</sup>/Df(2L)clot7*;  $n = 3$ ) has no significant impact on this response ( $p = 0.2151$ ). As a control of suppressed macroautophagy, knockdown of Atg1 (CG-Gal4;UAS-dsAtg1;  $n = 3$ ) leads to a significant inhibition of autolysosome accumulation ( $p = 0.0005$ ). Scale bar represents 50  $\mu$ M.

All data are shown as mean + SD. Complete statistics can be found in the [Supplemental Experimental Procedures](#) under “Statistical Information for Figures.”



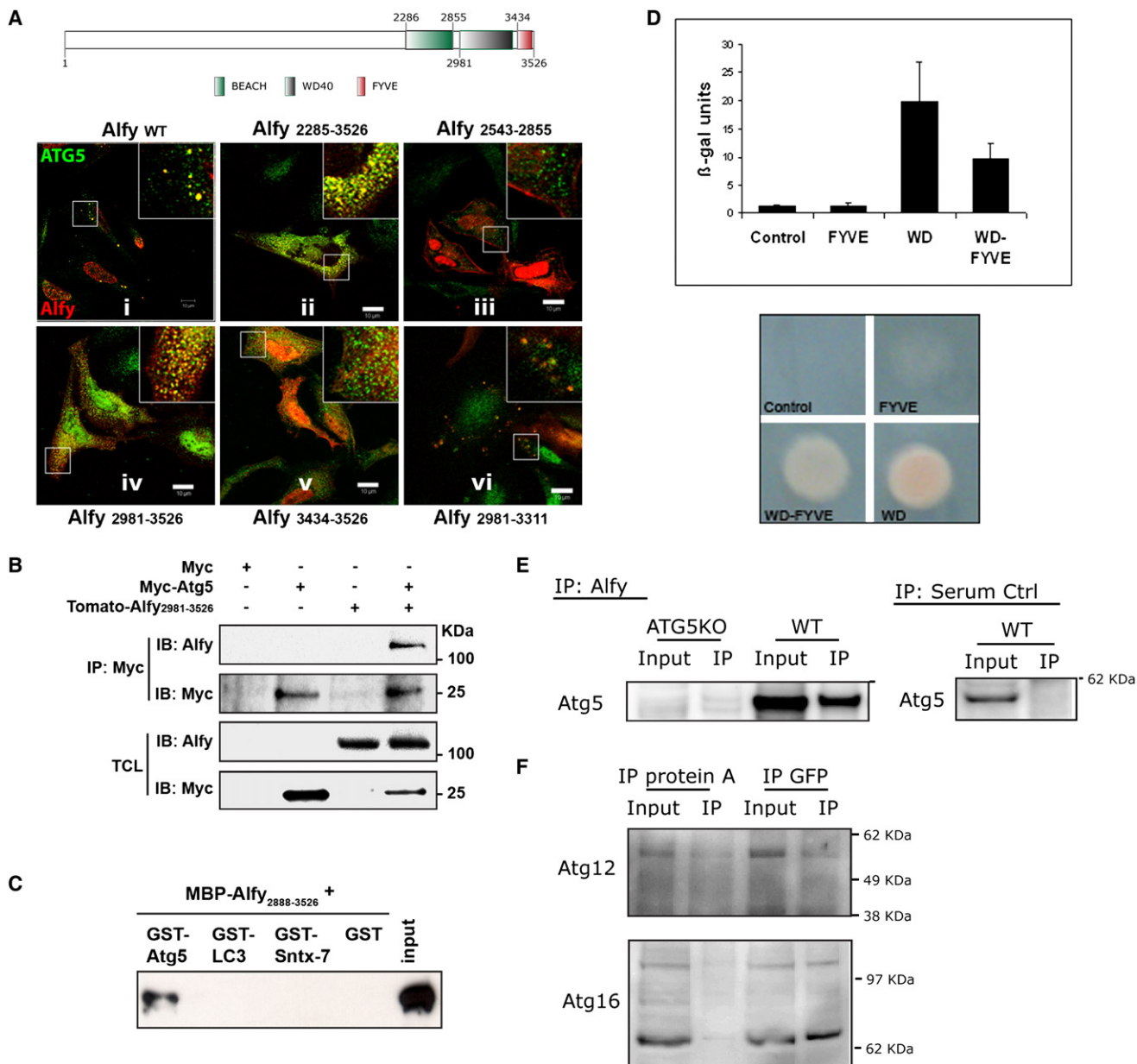


**Figure 4. Alfy Interacts Directly with Atg5**

(A) Schematic figure of Alfy noting the location of its BEACH domain, WD-40 repeats, and FYVE domain. Numbers indicate amino acids. Endogenous Alfy (red) colocalizes with endogenous Atg5 (green, panel i) in nonstarved HeLa cells. Constructs containing the WD-40 repeats (amino acids 3095–3436) colocalized with Atg5 (ii, iv, and vi). Expression of neither BEACH (iii) nor FYVE domains (v) alone led to Atg5 colocalization.

(B) Alfy C terminus and Atg5 can be found in the same complex in cell lysates. HeLa cells were cotransfected with the indicated plasmids, subjected to IP using anti-myc antibodies, and then probed with anti-Alfy or anti-myc antibodies.

(C) Atg5 directly interacts with the WD-40 repeats of Alfy as determined by GST pull-down. GST, GST-Atg5, GST-LC3, or GST-Syntaxin-7 were immobilized on prewashed beads and then incubated with MBP-Alfy<sub>2888–3526</sub>. Bound proteins were eluted and analyzed by immunoblotting against Alfy.

(D) Atg5-Alfy interaction revealed by Y2H. The yeast reporter strain L40 was cotransformed with pLexA-Atg5 and the indicated pGAD-Alfy plasmids. As a negative control, the strain was transformed with the plasmids pLexA-Atg5 and pGAD-GH. A positive interaction was detected in yeast coexpressing Gal4 activation domain fused to the WD40 repeats of Alfy together with the reporter activation sequence binding LexA-Atg5 fusion, as shown by  $\beta$ -galactosidase activities (top) and *HIS3* activities (bottom). Reporter activity in yeast expressing the FYVE domain alone was similar to controls. The values of  $\beta$ -galactosidase units are represented as mean  $\pm$  SD;  $n = 4$ .

(E) Endogenous Alfy can be found in a complex with endogenous Atg5-Atg12 in WT mouse embryonal fibroblasts (MEFs), but not in ATG5 knockout MEFs. Whole-cell lysates generated from MEFs were subject to IP using Rb anti-Alfy antibody serum and were probed for Atg5. Serum controls in WT MEFs were also negative for Atg5.

(F) Atg12 and Atg16L can also be found in a complex with Alfy. Whole-cell lysates generated from Htt103Q-mCFP cells were immunoprecipitated with GFP or with protein A beads as a negative control.



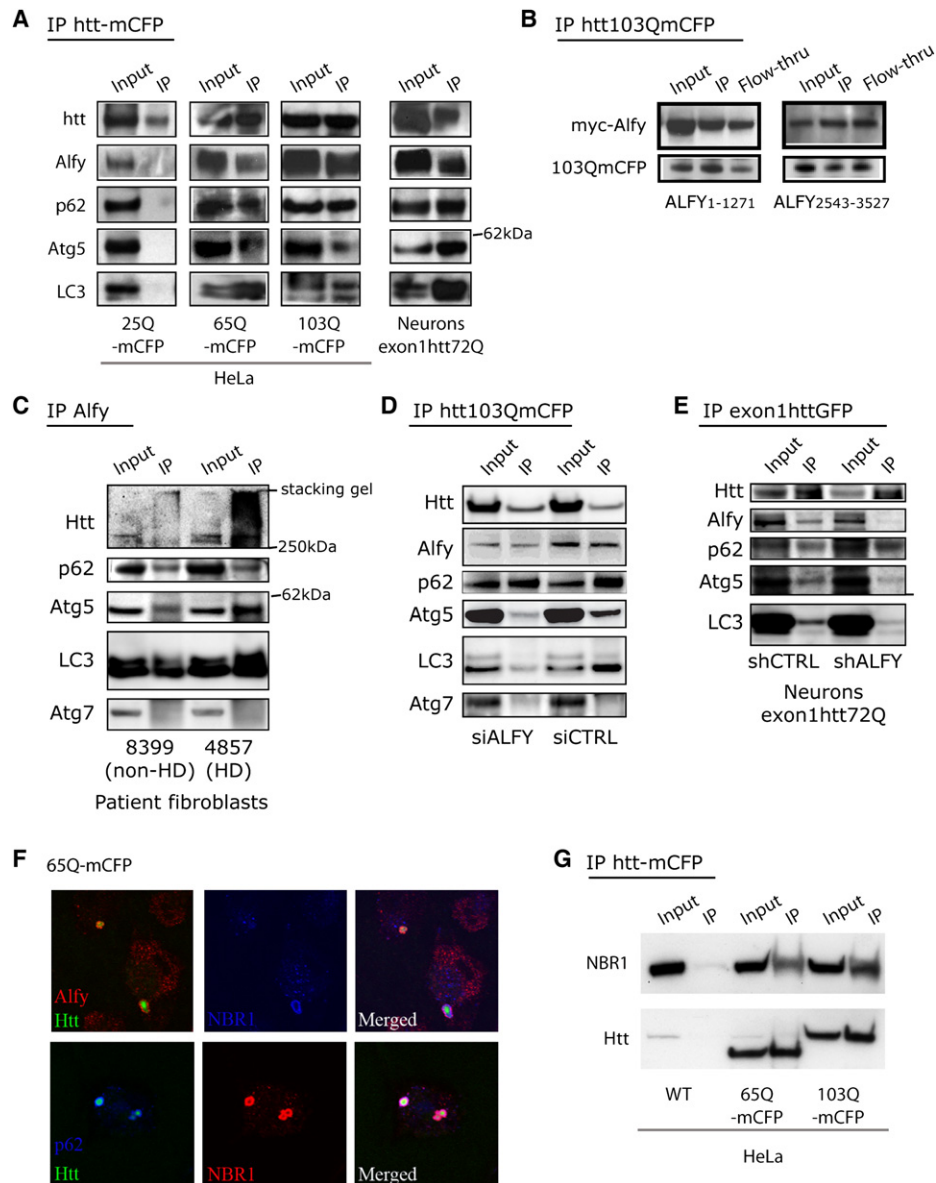


**Figure 5. Alfy Is in a Complex with the Aggregation-Prone Mutant Huntingtin Protein and Endogenous Atg5, p62, NBR1, and LC3**

(A) Co-IP experiments from whole-cell lysates from stable cell lines or primary neuronal model of HD. Lysates from stable cell lines Htt25Q-, Htt65Q-, and Htt103Q-mCFP were first immunoprecipitated via the CFP tag of the exon1Htt protein; were then probed for endogenous proteins with antibodies against Alfy, p62, Atg5, Atg7, and LC3; and were re-probed for Htt. Primary neurons transduced with lentivirus carrying exon1Htt72Q-GFP were first immunoprecipitated for Htt; were then probed with antibodies against Alfy, p62, and LC3; and were re-probed for Htt.

(B) Both a myc-tagged N-terminal and C-terminal fragment of Alfy co-IPs with exon1Htt-mCFP. Htt103Q-mCFP was immunoprecipitated with an antibody against GFP that also recognizes the mCFP tag.

(C) Co-IP experiments with anti-Alfy serum from whole-cell lysates from control or HD patient fibroblasts. In HD patient samples, Alfy co-IP with the mutant huntingtin protein, p62, Atg5, and LC3, but not with Atg7. Alfy still co-IPs p62, Atg5, and LC3 in unaffected patient samples, suggesting that there are non-HD aggregates that may be recognized by Alfy.

(D and E) Alfy is required for bringing Atg5 and LC3 to the complex. Experiments were performed similarly to (B) but after transfection with siRNA or shRNA against Alfy or a Ctrl sequence.

(D) Htt103Q-mCFP cell line.

(E) Primary rat cortical neurons. Immunoblotting (with antibodies against GFP, Alfy, p62, Atg5, and LC3) were all performed on the same blot. Based on the Htt input levels, transduction efficiency for (F) was not as efficient as in (B). All IP experiments are representative images from at least three independent experiments.

(F) Endogenous Alfy, p62, and NBR1 all localize to 65Q-mCFP aggregates.

(G) NBR1 forms a complex with the aggregation-prone mutant huntingtin protein. Htt65Q- and Htt103Q-mCFP were immunoprecipitated, and the blot was probed for NBR1.

aid the stable association of LC3 with p62 or that LC3 interacts through another region of Alfy.

Although the Htt fragment used in heterologous systems can effectively model protein aggregation, the full-length Htt protein is also known to aggregate in HD. We therefore determined whether Alfy plays a similar role under physiologic levels of Htt protein, using fibroblasts collected from HD and unaffected patients. Indeed, immunoprecipitation with Alfy revealed that endogenous Htt comes down with Alfy only in HD patient samples. Of interest, however, Atg5, LC3, and p62 are found in a complex with Alfy in both samples, indicating that the Alfy complex exists independently of Htt aggregation and thus may generalize across different aggregating proteins. To explore this further, we turned to a non-polyQ protein known to form cellular aggregates,  $\alpha$ -synuclein ( $\alpha$ -Syn), with and without its more aggregation-prone mutation, A53T (Figure S6C). Although the soluble form of  $\alpha$ -Syn can be degraded by chaperone-mediated autophagy (Cuervo et al., 2004; Vogiatzi et al., 2008), its aggregated form may be degraded by macroautophagy (Sarkar et al., 2007). Confocal microscopy and filter trap analysis revealed that, in these cell lines, both  $\alpha$ -Syn-mCFP and  $\alpha$ -Syn(A53T)-mCFP form aggregates, although more frequently in the latter (Figures S6C and S6D). Consistent with polyQ aggregate clearance, filter trap analysis revealed that Alfy KD inhibited the ability of the cells to eliminate the SDS-insoluble  $\alpha$ -Syn proteins, and co-IP analysis found that Alfy and Atg5 precipitated with the synuclein proteins (Figure S6E). Taken together, these data suggest that Alfy is required for the elimination of different types of aggregated proteins.

Recently, NBR1 was found to cooperate with p62 in the sequestration of misfolded ubiquitinated proteins for degradation by autophagy (Kirkin et al., 2009). Both proteins have a ubiquitin-binding UBA domain and LC3-interacting regions (LIR). Because we found that Alfy makes a complex with p62-positive polyQ protein (Figures 5A, 5D, and 5E), we also pursued NBR1. NBR1 colocalized with Alfy and polyQ inclusions and was found to co-IP with mutant Htt polyQ proteins (Figures 5F and 5G). Overall, this suggested that polyQ protein can interact with p62 and NBR1, and Alfy may target these proteins for degradation.

### Alfy Overexpression Can Enhance Aggregate Clearance in a Primary Neuronal Model of HD

We have found that Alfy is required for aggregate clearance, and it may do so by scaffolding the macroautophagy machinery through its C terminus. Of interest, we generally noticed fewer polyQ inclusions upon ectopic expression of the C-terminal fragment of Alfy, and we therefore speculated that, by increasing Alfy expression, we may increase mutant Htt elimination and, in turn, abrogate toxicity of mutant Htt. Htt103Q-mCFP cells were transiently transfected with the C terminus of Alfy containing the WD-40 repeats and the FYVE domain (Alfy<sub>2981–3526</sub>). Quantification of the number of cells containing inclusions revealed that overexpression of this fragment indeed enhanced clearance of polyQ aggregates, but not in cells depleted of Atg5 (Figure S7A). Moreover, mutagenesis throughout the WD-40 repeat of this construct (4 W mutated to A) also inhibited inclusion clearance, indicating that clearance is dependent on Atg5 binding to Alfy (Figure S7A).

To determine whether overexpression of Alfy can diminish the level of mutant Htt aggregates in a nondividing cell, we used the neuronal model of HD that we described for Figure 5. Neurons were transduced at day in vitro (DIV) 2 and were transfected with different Tomato-tagged Alfy constructs 5 days later, after the appearance of inclusions. Cells were then fixed 72 hr post-transfection and examined for the presence or absence of inclusions. As shown in Figure 6A, transduced neurons demonstrated robust staining of exon1Htt72Q-GFP, and inclusions were found in the soma as well as within the processes of the neurons. Protein also accumulated within the nucleus, as has previously been reported; however, due to the intensity of the staining, it was unclear whether discrete puncta could be observed. Although transfection of an N terminal (Alfy<sub>1–1271</sub>) or internal (Alfy<sub>2285–2981</sub>) portion of Alfy had no effect on aggregation, overexpression of the C-terminal fragment of Alfy (Alfy<sub>2981–3526</sub>) led to a significant reduction of protein aggregates in the neurons (Figures 6A and 6B). Similar to our finding in HeLa cells, colocalization of Alfy<sub>1–1271</sub> with Htt inclusions could also be observed (Figure S7B). Overexpression of the full-length 400 kDa Alfy was very difficult to achieve, but in the few cells that were successfully transfected, the frequency of inclusions was fewer (Figure S7C). These data indicate that overexpression of Alfy or the C-terminal of Alfy can diminish protein accumulation, further supporting that Alfy is required for clearance of aggregates by acting as a scaffold for the macroautophagic machinery.

### Alfy/Bchs Overexpression Is Neuroprotective in a Fly-Eye Model of HD

To determine whether enhanced Alfy/Bchs expression can be neuroprotective, we assessed the impact of overexpressing Bchs in an established *Drosophila* eye model of polyglutamine toxicity (Kazemi-Esfarjani and Benzer, 2000). For this study, we used the bipartate Gal4/UAS system to drive expression of a UAS-polyQ127 transgene in the developing fly eye (*pGMR-Gal4*). As previously shown, this genotype (*Gal4, UAS-polyQ127*) generates a phenotype that includes a reduced eye size, pigmentation loss, and ommatidial disorganization, as well as the formation of necrotic regions (Figure 6C, arrows). This model has successfully identified genetic modifiers of polyglutamine toxicity (Bilen and Bonini, 2005; Kazemi-Esfarjani and Benzer, 2000; Lam et al., 2006; Pandey et al., 2007; Steffan et al., 2001).

Quantification of the number of necrotic areas revealed a significant degree of protection due to coexpression of full-length *bchs* (*UAS-FL-Bchs*) or C-terminal Bchs (*UAS-bchs-C1000*) with *UAS-polyQ127* (Figure 6D). This included the reduction or absence of necrosis and an overall improvement in eye size, morphology, and pigmentation. Of interest, overexpression of Bchs-C1000 produces a higher level of protection than the full-length protein. This may, in part, be due to the fact that enhanced expression of the large and complex 400 kDa Bchs protein produces its own external eye phenotype, as well as subcellular axonal trafficking defects within the eye (*GMR-Gal4, UAS-bchs*) (Figure S7D) (Simonsen et al., 2007).

To determine whether the Bchs-mediated protection required macroautophagy, we suppressed the pathway through depletion of Atg8a (*UAS-dsAtg8a-RNAi*). We have previously shown that the loss of Atg8a was sufficient to inhibit macroautophagy

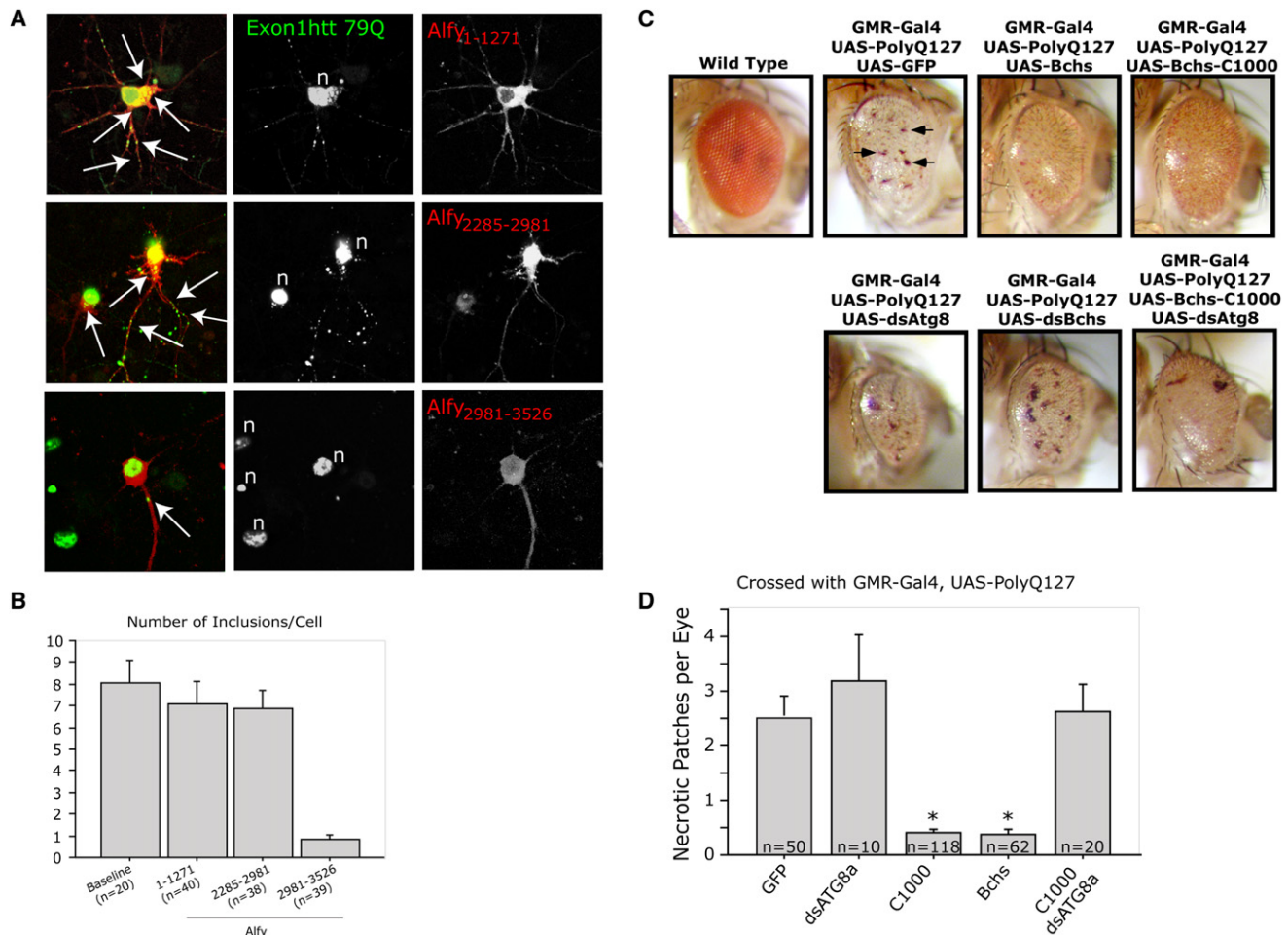


**Figure 6. Alfy/Bchs Overexpression Leads to a Disappearance of Inclusions in a Primary Neuronal Model of HD and Diminished Neurotoxicity in a *Drosophila* Eye Model of PolyQ Toxicity**

(A and B) Alfy overexpression in a lentiviral model of HD leads to fewer inclusions in rat primary cortical neurons.

(A) Immunofluorescence (IF) against exon1Htt (green) with MAB5492 reveals that transduced neurons exhibit robust aggregation throughout the cell, including the soma and processes (white arrows), and nuclei (n). Transfection of Alfy<sub>1-1271</sub> ( $p = 0.4241$ ) and Alfy<sub>2285-2981</sub> ( $p = 0.3325$ ) had no noticeable effect on the number of inclusions/cell. In contrast, expression of Alfy<sub>2981-3526</sub> led to a significant reduction in the aggregate load in the neurons ( $p < 0.001$ ). The visible green puncta in the field that do not colocalize with red are attributable to neuronal processes from non-Alfy transfected neurons.

(B) Number of inclusions per cell was counted in the number of cells indicated. All visible puncta within a 100  $\mu\text{m}$  radius from the center of the nucleus were counted. Cells were considered within the cell if the puncta (green) colocalized to cytosol expressing the Tomato fluorophore (red).

(C and D) Alfy/Bchs overexpression in the *Drosophila* eye leads to protection against polyQ toxicity.

(C) Canton-S control flies (wild-type) show the normal pigmentation profiles and ommatidial features of the adult *Drosophila* eye. Expression of polyQ127 peptide (UAS-PolyQ-127;  $n = 20$ ) using the pGMR-Gal4 driver leads to distinctive defects throughout the eye, including necrotic regions (pGMR-Gal4/UAS-PolyQ-127, arrows;  $n = 20$ ). Coexpression of full-length Bchs (pGMR-Gal4, UAS-PolyQ-127/UAS-EP-bchs;  $n = 20$ ) reduced the level of observable necrosis. Coexpression of PolyQ127 peptide with the C-terminal region of Bchs (pGMR-Gal4, UAS-PolyQ-127/UAS-bchs-C1000;  $n = 20$ ) leads to suppression of this external toxic phenotypes. Coexpression of a dsAtg8a (pGMR-Gal4, UAS-PolyQ-127/UAS-bchs-C1000/UAS-dsAtg8a;  $n = 15$ ) RNAi transgene blocked this protective effect.

(D) The number of necrotic regions was determined for (C). Whereas coexpression of dsAtg8a further reduced eye size, it did not significantly alter necrosis levels ( $p = 0.2391$ ). Both full-length and C1000-Bchs significantly reduced fly eye necrosis ( $p < 0.0001$ ). This decrease was abrogated when C1000 was coexpressed with a dsRNA against ATG8a ( $p = 0.9977$ ), which significantly inhibits macroautophagy in the developing eye.

All data are shown as mean + SE. Complete statistics can be found in [Supplemental Experimental Procedures](#) under "Statistical Information for Figures."

in adult *Drosophila* head and that Atg8b is not expressed in this tissue (Simonsen et al., 2008). When the C-terminal Bchs was expressed together with Atg8a KD using a UAS-dsAtg8a transgene, the protection against polyQ127 generated by higher Bchs-C1000 levels was no longer observed (Figures 6C and 6D). Western analysis of polyQ127 peptide levels prepared

from the different fly genotypes showed that changes in eye phenotypes were not due to altered expression of the transgene (Figure S7E). This set of experiments indicates that the Alfy/Bchs proteins have a significant role in suppressing the in vivo cytotoxicity of aggregation-prone proteins, in large part mediated through the macroautophagic pathway.



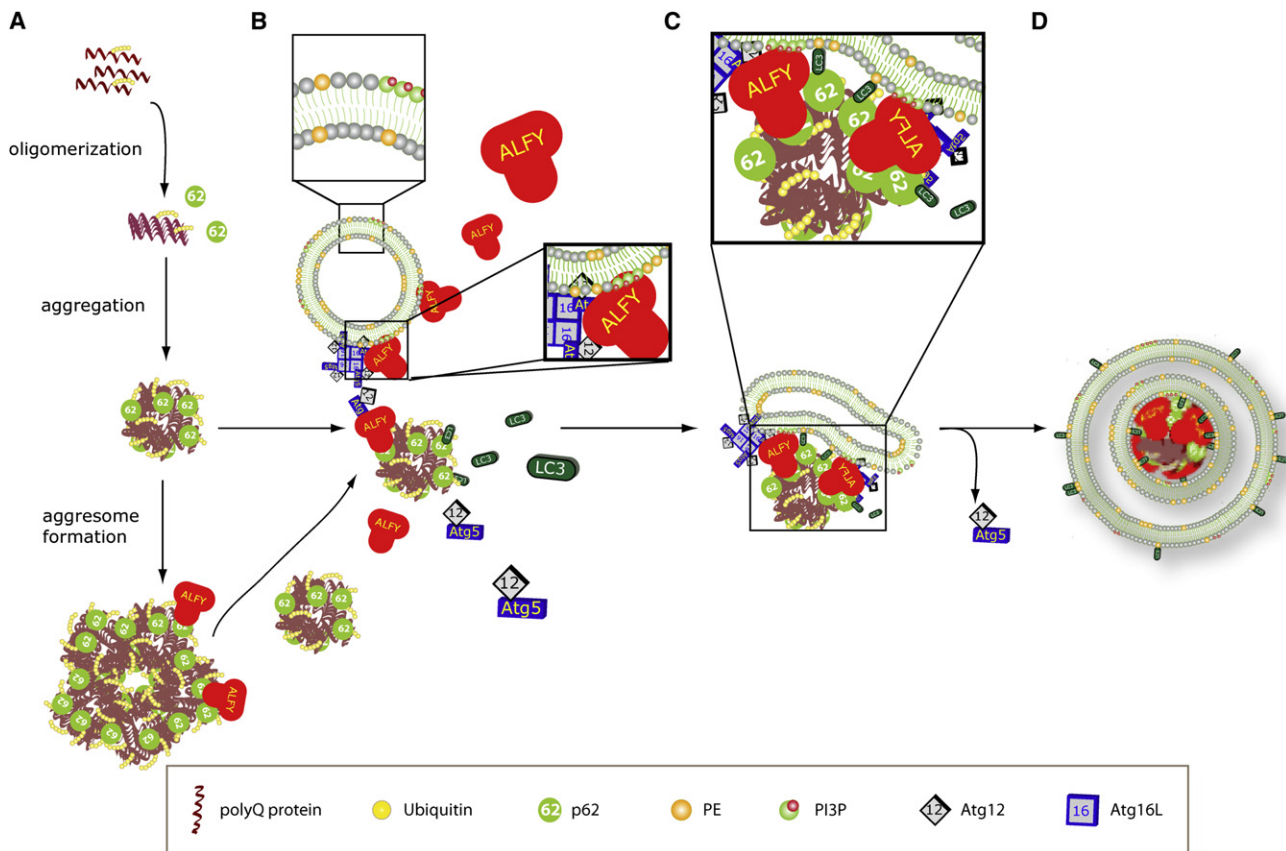


**Figure 7. Proposed Model of Alfy-Mediated Clearance of Protein Aggregates**

(A) Expression of expanded polyQ proteins leads to their polyubiquitination, accumulation, and aggregation. The ubiquitinated protein can be recognized by p62. (B) In the presence of aggregating protein, Alfy translocates from the nucleus into the cytosol, where it interacts with PI3P-containing membranes through its FYVE domain, Atg5-Atg12 through its WD-40 domain, and the ubiquitin- and p62-positive protein. p62, which interacts directly with LC3, may bring unbound LC3 to the inclusion as well. (C) Alfy brings the different components together, permitting Atg5-Atg12-Atg16L to aid the conversion of LC3 to its PE-bound form. It is uncertain whether p62 binds free LC3, PE-bound LC3, or both; however, interaction with PE-bound LC3 may help stabilize the membrane around the aggregate. Atg5-Atg12 possibly leaves as LC3 conjugation occurs along the membrane. (D) Aggregates are packaged into autophagosomes to permit eventual degradation upon fusion to the lysosome. Not to scale.

## DISCUSSION

In this study, we have found that Alfy is required for the macroautophagic elimination of aggregated proteins, but not for macroautophagic elimination of bulk cytosol in response to starvation. We propose that Alfy functions as a scaffold that brings together the E3-like ligase, Atg5-Atg12-Atg16L, and LC3 to the target substrate to permit the degradation of expanded polyglutamine proteins in different cell types, including neurons. Finally, we have found that its overexpression can enhance the elimination of toxic polyglutamine proteins in a primary neuronal model and permit protection in a *Drosophila* eye model of polyQ toxicity.

The role of the lysosome and its capacity to eliminate aggregated proteins of expanded polyQ proteins has been explored extensively (Iwata et al., 2005a; Ravikumar et al., 2004; Yamamoto et al., 2006). It has remained a question, however, how they are targeted to the autophagosome for degradation. Our

findings demonstrate that Alfy plays an important role in this process, and we suggest the following model (Figure 7): as the polyQ protein is expressed and accumulates, it evolves from oligomers to increasingly larger aggregates to inclusions. The polyubiquitinated forms of the accumulating mutant protein are recognized by p62, which may aid aggregate growth via self-polymerization of its PB1 domain (Bjørkøy et al., 2005), together with previously implicated microtubule- and HDAC6-dependent mechanisms (Iwata et al., 2005b; Johnston et al., 1998; Kawaguchi et al., 2003). Meanwhile, in the presence of aggregation-prone proteins, Alfy is transported from the nucleus to the cytoplasm, where it may interact with PI3P-containing membranes through its FYVE domain (Simonsen et al., 2004) and Atg5-Atg12 through its WD-40 domain. Although drawn as a vesicle, the membrane source for the autophagosome is still unclear, although the ER (Axe et al., 2008; Hayashi-Nishino et al., 2009; Ylä-Anttila et al., 2009) has been implicated. Once at the membrane, Atg5-Atg12 can interact with Atg16L (Fujita

et al., 2008; Mizushima et al., 2003). Alfý also interacts with aggregated polyQ proteins, most likely through its interaction with p62 (Claussen et al., 2010). In this manner, we speculate that Alfý brings a membrane source and Atg5-Atg12-Atg16L to the inclusion so that they can act as part of a greater E3 ligase-like complex for LC3 (Hanada et al., 2007). The presence of p62 may stabilize the lipid-bound LC3, thus permitting the autophagosome to build directly around the inclusion. Although giant (diameter > 1  $\mu$ m) inclusions were not found frequently in double-membrane structures by immuno-EM, the large inclusions contained were much larger than the usual 100 nm size AVs. Clearly, further in vitro and in vivo experiments must be performed to test this model directly.

This selective sorting of cargo in macroautophagy is reminiscent of protein trafficking from endocytosis to secretion, for which particular cargo are directed to unique trafficking fates. Recently, in yeast, Atg32 has been shown to confer selectivity during mitophagy (Kanki et al., 2009; Okamoto et al., 2009). In mammalian systems, several proteins that link the autophagic machinery to its substrates have been identified. Termed “autophagy receptors,” they are involved in degradation of ubiquitinated bacteria (NDP52) (Thurston et al., 2009), mitochondria (NIX) (Novak et al., 2010; Sandoval et al., 2008), and protein aggregates (p62 and NBR1) (Kirkin et al., 2009; Pankiv et al., 2007). All proteins contain an LIR and substrate recognition domain. Because Alfý interacts with p62 (Claussen et al., 2010), it will be interesting to determine how Alfý influences the degradation of other autophagy receptor proteins and their cargo.

Our findings indicate that an innate cellular process to package protein aggregates into autophagic vacuoles exists in mammalian cells. Several results echo the Cvt (cytosol-to-vacuole targeting) pathway in yeast (Nair and Klionsky, 2005). Our ultrastructural studies show that relatively large aggregated structures can be found sequestered in double-membrane vesicles, devoid of bulk cytosol. Further, the clearance of aggregated proteins clearly requires the macroautophagic machinery but, like Cvt, also requires additional unique factors to act as a scaffold between the cargo aggregate and the membrane building machinery. Aggregation of the cargo may, therefore, be one of the first steps toward degradation, and hence inhibition thereof may confer toxicity because the protein can no longer be eliminated. This may explain studies indicating the “protective” nature of inclusions in neurons (Arrasate et al., 2004; Taylor et al., 2003). Nonetheless, if, indeed, a Cvt-like process exists, why is there a prevalence of protein accumulation in human disease? Do levels of Alfý relate to the susceptibility to protein aggregation? We have previously shown that Alfý is ubiquitously expressed in mouse tissue, with highest levels found in brain (Simonsen et al., 2004). In *Drosophila*, expression level of the Alfý homolog *bchs* is highest in neurons. Alfý/*bchs* may be especially important in nondividing cells, which require more “help” to clear aggregate-prone or aggregated proteins to prevent accumulation of protein aggregates. Consistent with this are previously published studies demonstrating that loss of *Bchs* leads to the accumulation of ubiquitinated proteins in fly neurons (Finley et al., 2003). Our complementary experiment using overexpression of Alfý in neurons shows that increased

levels of Alfý or its C terminus permit clearance (Figures 6 and S7A), suggesting that Alfý may be rate limiting to the degradation of aggregated proteins. This may be linked to the prospect that Alfý can corral key members of the macroautophagy machinery, and thus its constitutive presence may limit the starvation response, leading to cell death. To avoid this possibility, the nuclear localization of Alfý may limit its bioavailability. This hypothesis and how cellular stress permits Alfý to exit the nucleus is under current investigation.

## EXPERIMENTAL PROCEDURES

Complete methods can be found in the [Supplemental Experimental Procedures](#). Human fibroblasts were obtained with permission from Coriell Cell Repositories.

### Promoter Shutdown Experiments and Filter Trap Assay

At 48 hr after siRNA transfection, HttPolyQ-mCFP cells were exposed to 100 ng/ml dox for 3 days to permit more than 50% of clearance. The effect of siRNAs on aggregate clearance was analyzed by confocal quantification as described (Yamamoto et al., 2006) or by membrane filter trap assay as previously published (Bailey et al., 2002; Passani et al., 2000; Wanker et al., 1999).

### Long-Lived Protein Degradation Assay

Cells were labeled overnight with [ $^{14}$ C]valine, chased in fresh media with excess valine overnight, and then incubated for 4 hr with complete media (CM) or starvation media (HBSS/EBSS + 10mM HEPES, Starv). To ensure that protein degradation during nutrient deprivation was due to macroautophagy, experiments were also performed in the presence of 3MA. LLP degradation was monitored 72 hr posttransfection.

### Autolysosome Assay in *Drosophila* Fat Body Cells

Performed as previously described (Rusten et al., 2004). In brief, second instar larvae were fed or starved on limited medium (3 hr sucrose-only medium). Fat bodies from individual larvae were dissected, stained with LR (Molecular Probes), and immediately imaged by confocal microscopy. The number of autolysosomes in fat tissue was quantified from replicate 50  $\mu$ m<sup>2</sup> areas. Information on *Drosophila* lines and genetic crosses can be found in the [Supplemental Experimental Procedures](#).

### Primary Neuronal Model of HD

Primary rat cortical neurons were plated at E18. Neurons were transduced with lentivir carrying exon1Htt with 72Q on DIV2. Alfý constructs were transiently introduced at DIV7. Neurons were fixed and stained 72 hr later.

### Quantification of Necrotic Eye Regions in *Drosophila* Eye Model

Crosses were maintained at 25°C, replicate eyes from individual genotypes were examined, and the average number of necrotic regions were counted and SEM calculated. Multiple representative digital images were taken from each genotype using a Leica MZ6 dissecting microscope and Nikon Coolpix 990 camera system. Information on lines and genetic crosses can be found in the [Supplemental Experimental Procedures](#).

### Statistical Analyses

Statistical analyses were performed using Statview 5.0 (SAS Institute). Images were processed using Adobe Photoshop 7.0 and 8.0. Complete statistical analyses can be found in the [Supplemental Experimental Procedures](#).

## SUPPLEMENTAL INFORMATION

Supplemental Information includes Supplemental Experimental Procedures and seven figures and can be found with this article online at [doi:10.1016/j.molcel.2010.04.007](https://doi.org/10.1016/j.molcel.2010.04.007).

## ACKNOWLEDGMENTS

This study was supported by the NINDS RO1 NS050199 (M.A., K.M.M., A.Y.), NINDS RO1 NS063973 (T.J.M., A.Y.), Parkinson's Disease Foundation (K.M.M., A.Y.), Hereditary Disease Foundation (A.Y.), NIH/NIA R21 AG030187 (K.D.F.), the FUGE Programme of the Research Council of Norway (P.I., T.L., A.B., H.S., A.S.), and the Norwegian Cancer Society (A.S.). We would like to thank Drs. R. Kopito and T. Yoshimori for their anti-LC3 antibodies and Drs. N. Mizushima for the ATG5 KO MEFs and S.A. Tooze for HEK293 LC3-GFP cells. The UAS-PolyQ127 line was a gift from Seymour Benzer. The cryo EM was performed at the New York Structural Biology Center.

Received: April 5, 2009

Revised: November 6, 2009

Accepted: April 2, 2010

Published: April 22, 2010

## REFERENCES

- Arrasate, M., Mitra, S., Schweitzer, E.S., Segal, M.R., and Finkbeiner, S. (2004). Inclusion body formation reduces levels of mutant huntingtin and the risk of neuronal death. *Nature* 431, 805–810.
- Axe, E.L., Walker, S.A., Maniava, M., Chandra, P., Roderick, H.L., Habermann, A., Griffiths, G., and Ktistakis, N.T. (2008). Autophagosome formation from membrane compartments enriched in phosphatidylinositol 3-phosphate and dynamically connected to the endoplasmic reticulum. *J. Cell Biol.* 182, 685–701.
- Bailey, C.K., Andriola, I.F., Kamping, H.H., and Merry, D.E. (2002). Molecular chaperones enhance the degradation of expanded polyglutamine repeat androgen receptor in a cellular model of spinal and bulbar muscular atrophy. *Hum. Mol. Genet.* 11, 515–523.
- Berg, T.O., Fengsrud, M., Strömhaug, P.E., Berg, T., and Seglen, P.O. (1998). Isolation and characterization of rat liver amphisomes. Evidence for fusion of autophagosomes with both early and late endosomes. *J. Biol. Chem.* 273, 21883–21892.
- Bilen, J., and Bonini, N.M. (2005). Drosophila as a model for human neurodegenerative disease. *Annu. Rev. Genet.* 39, 153–171.
- Bjørkøy, G., Lamark, T., Brech, A., Outzen, H., Perander, M., Overvatn, A., Stenmark, H., and Johansen, T. (2005). p62/SQSTM1 forms protein aggregates degraded by autophagy and has a protective effect on huntingtin-induced cell death. *J. Cell Biol.* 171, 603–614.
- Boland, B., and Nixon, R.A. (2006). Neuronal macroautophagy: from development to degeneration. *Mol. Aspects Med.* 27, 503–519.
- Claussen, T.H., Lamark, T., Isakson, P., Finley, K., Brech, A., Overvatn, A., Stenmark, H., Bjørkøy, G., Johansen, T., and Simonsen, A. (2010). p62/SQSTM1 and Alf1 interact to facilitate formation of ubiquitinated protein aggregates that become degraded by autophagy. *Autophagy* 6, 1–15.
- Cornett, J., Cao, F., Wang, C.E., Ross, C.A., Bates, G.P., Li, S.H., and Li, X.J. (2005). Polyglutamine expansion of huntingtin impairs its nuclear export. *Nat. Genet.* 37, 198–204.
- Cuervo, A.M., Stefanis, L., Fredenburg, R., Lansbury, P.T., and Sulzer, D. (2004). Impaired degradation of mutant alpha-synuclein by chaperone-mediated autophagy. *Science* 305, 1292–1295.
- Davies, S.W., Turmaine, M., Cozens, B.A., DiFiglia, M., Sharp, A.H., Ross, C.A., Scherzinger, E., Wanker, E.E., Mangiarini, L., and Bates, G.P. (1997). Formation of neuronal intranuclear inclusions underlies the neurological dysfunction in mice transgenic for the HD mutation. *Cell* 90, 537–548.
- DiFiglia, M., Sapp, E., Chase, K.O., Davies, S.W., Bates, G.P., Vonsattel, J.P., and Aronin, N. (1997). Aggregation of huntingtin in neuronal intranuclear inclusions and dystrophic neurites in brain. *Science* 277, 1990–1993.
- Filimonenko, M., Stuffers, S., Raiborg, C., Yamamoto, A., Malerød, L., Fisher, E.M., Isaacs, A., Brech, A., Stenmark, H., and Simonsen, A. (2007). Functional multivesicular bodies are required for autophagic clearance of protein aggregates associated with neurodegenerative disease. *J. Cell Biol.* 179, 485–500.
- Finley, K.D., Edeen, P.T., Cumming, R.C., Mardahl-Dumesnil, M.D., Taylor, B.J., Rodriguez, M.H., Hwang, C.E., Benedetti, M., and McKeown, M. (2003). Blue cheese mutations define a novel, conserved gene involved in progressive neural degeneration. *J. Neurosci.* 23, 1254–1264.
- Fujita, N., Itoh, T., Omori, H., Fukuda, M., Noda, T., and Yoshimori, T. (2008). The Atg16L complex specifies the site of LC3 lipidation for membrane biogenesis in autophagy. *Mol. Biol. Cell* 19, 2092–2100.
- Hanada, T., Noda, N.N., Satomi, Y., Ichimura, Y., Fujioka, Y., Takao, T., Inagaki, F., and Ohsumi, Y. (2007). The ATG12-ATG5 conjugate has a novel e3-like activity for protein lipidation in autophagy. *J. Biol. Chem.* 282, 37298–37302.
- Hayashi-Nishino, M., Fujita, N., Noda, T., Yamaguchi, A., Yoshimori, T., and Yamamoto, A. (2009). A subdomain of the endoplasmic reticulum forms a cradle for autophagosome formation. *Nat. Cell Biol.* 11, 1433–1437.
- Hosokawa, N., Hara, Y., and Mizushima, N. (2006). Generation of cell lines with tetracycline-regulated autophagy and a role for autophagy in controlling cell size. *FEBS Lett.* 580, 2623–2629.
- Iwata, A., Christianson, J.C., Bucci, M., Ellerby, L.M., Nukina, N., Forno, L.S., and Kopito, R.R. (2005a). Increased susceptibility of cytoplasmic over nuclear polyglutamine aggregates to autophagic degradation. *Proc. Natl. Acad. Sci. USA* 102, 13135–13140.
- Iwata, A., Riley, B.E., Johnston, J.A., and Kopito, R.R. (2005b). HDAC6 and microtubules are required for autophagic degradation of aggregated huntingtin. *J. Biol. Chem.* 280, 40282–40292.
- Johnston, J.A., Ward, C.L., and Kopito, R.R. (1998). Aggresomes: a cellular response to misfolded proteins. *J. Cell Biol.* 143, 1883–1898.
- Kabeya, Y., Mizushima, N., Ueno, T., Yamamoto, A., Kirisako, T., Noda, T., Kominami, E., Ohsumi, Y., and Yoshimori, T. (2000). LC3, a mammalian homologue of yeast Apg8p, is localized in autophagosome membranes after processing. *EMBO J.* 19, 5720–5728.
- Kanki, T., Wang, K., Cao, Y., Baba, M., and Klionsky, D.J. (2009). Atg32 is a mitochondrial protein that confers selectivity during mitophagy. *Dev. Cell* 17, 98–109.
- Kawaguchi, Y., Kovacs, J.J., McLaurin, A., Vance, J.M., Ito, A., and Yao, T.P. (2003). The deacetylase HDAC6 regulates aggresome formation and cell viability in response to misfolded protein stress. *Cell* 115, 727–738.
- Kazemi-Esfarjani, P., and Benzer, S. (2000). Genetic suppression of polyglutamine toxicity in Drosophila. *Science* 287, 1837–1840.
- Kirkin, V., Lamark, T., Sou, Y.S., Bjørkøy, G., Nunn, J.L., Bruun, J.A., Shvets, E., McEwan, D.G., Clausen, T.H., Wild, P., et al. (2009). A role for NBR1 in autophagosomal degradation of ubiquitinated substrates. *Mol. Cell* 33, 505–516.
- Klionsky, D.J. (2005). Autophagy. *Curr. Biol.* 15, R282–R283.
- Klionsky, D.J., Abeliovich, H., Agostinis, P., Agrawal, D.K., Aliev, G., Askew, D.S., Baba, M., Baehrecke, E.H., Bahr, B.A., Ballabio, A., et al. (2008). Guidelines for the use and interpretation of assays for monitoring autophagy in higher eukaryotes. *Autophagy* 4, 151–175.
- Köchl, R., Hu, X.W., Chan, E.Y., and Tooze, S.A. (2006). Microtubules facilitate autophagosome formation and fusion of autophagosomes with endosomes. *Traffic* 7, 129–145.
- Lam, Y.C., Bowman, A.B., Jafar-Nejad, P., Lim, J., Richman, R., Fryer, J.D., Hyun, E.D., Duvick, L.A., Orr, H.T., Botas, J., and Zoghbi, H.Y. (2006). ATAXIN-1 interacts with the repressor Capicua in its native complex to cause SCA1 neuropathology. *Cell* 127, 1335–1347.
- Lindmo, K., Simonsen, A., Brech, A., Finley, K., Rusten, T.E., and Stenmark, H. (2006). A dual function for Deep orange in programmed autophagy in the Drosophila melanogaster fat body. *Exp. Cell Res.* 312, 2018–2027.
- Marzella, L., Ahlberg, J., and Glaumann, H. (1982). Isolation of autophagic vacuoles from rat liver: morphological and biochemical characterization. *J. Cell Biol.* 93, 144–154.
- Mizushima, N., Kuma, A., Kobayashi, Y., Yamamoto, A., Matsubae, M., Takao, T., Natsume, T., Ohsumi, Y., and Yoshimori, T. (2003). Mouse Apg16L, a novel



- WD-repeat protein, targets to the autophagic isolation membrane with the App12-App5 conjugate. *J. Cell Sci.* 116, 1679–1688.
- Nair, U., and Klionsky, D.J. (2005). Molecular mechanisms and regulation of specific and nonspecific autophagy pathways in yeast. *J. Biol. Chem.* 280, 41785–41788.
- Novak, I., Kirkin, V., McEwan, D.G., Zhang, J., Wild, P., Rozenknop, A., Rogov, V., Löhr, F., Popovic, D., Occhipinti, A., et al. (2010). Nix is a selective autophagy receptor for mitochondrial clearance. *EMBO Rep.* 11, 45–51.
- Okamoto, K., Kondo-Okamoto, N., and Ohsumi, Y. (2009). Mitochondria-anchored receptor Atg32 mediates degradation of mitochondria via selective autophagy. *Dev. Cell* 17, 87–97.
- Pandey, U.B., Nie, Z., Batlevi, Y., McCray, B.A., Ritson, G.P., Nedelsky, N.B., Schwartz, S.L., DiProspero, N.A., Knight, M.A., Schuldiner, O., et al. (2007). HDAC6 rescues neurodegeneration and provides an essential link between autophagy and the UPS. *Nature* 447, 859–863.
- Pankiv, S., Clausen, T.H., Lamark, T., Brech, A., Bruun, J.A., Outzen, H., Øvervatn, A., Bjørkøy, G., and Johansen, T. (2007). p62/SQSTM1 binds directly to Atg8/LC3 to facilitate degradation of ubiquitinated protein aggregates by autophagy. *J. Biol. Chem.* 282, 24131–24145.
- Passani, L.A., Bedford, M.T., Faber, P.W., McGinnis, K.M., Sharp, A.H., Gusella, J.F., Vonsattel, J.P., and MacDonald, M.E. (2000). Huntingtin's WW domain partners in Huntington's disease post-mortem brain fulfill genetic criteria for direct involvement in Huntington's disease pathogenesis. *Hum. Mol. Genet.* 9, 2175–2182.
- Ravikumar, B., Duden, R., and Rubinsztein, D.C. (2002). Aggregate-prone proteins with polyglutamine and polyalanine expansions are degraded by autophagy. *Hum. Mol. Genet.* 11, 1107–1117.
- Ravikumar, B., Vacher, C., Berger, Z., Davies, J.E., Luo, S., Oroz, L.G., Scaravilli, F., Easton, D.F., Duden, R., O'Kane, C.J., and Rubinsztein, D.C. (2004). Inhibition of mTOR induces autophagy and reduces toxicity of polyglutamine expansions in fly and mouse models of Huntington disease. *Nat. Genet.* 36, 585–595.
- Rockel, T.D., Stuhlmann, D., and von Mikecz, A. (2005). Proteasomes degrade proteins in focal subdomains of the human cell nucleus. *J. Cell Sci.* 118, 5231–5242.
- Rusten, T.E., Lindmo, K., Juhász, G., Sass, M., Seglen, P.O., Brech, A., and Stenmark, H. (2004). Programmed autophagy in the *Drosophila* fat body is induced by ecdysone through regulation of the PI3K pathway. *Dev. Cell* 7, 179–192.
- Sandoval, H., Thiagarajan, P., Dasgupta, S.K., Schumacher, A., Prchal, J.T., Chen, M., and Wang, J. (2008). Essential role for Nix in autophagic maturation of erythroid cells. *Nature* 454, 232–235.
- Sarkar, S., Perlstein, E.O., Imarisio, S., Pineau, S., Cordenier, A., Maglathlin, R.L., Webster, J.A., Lewis, T.A., O'Kane, C.J., Schreiber, S.L., and Rubinsztein, D.C. (2007). Small molecules enhance autophagy and reduce toxicity in Huntington's disease models. *Nat. Chem. Biol.* 3, 331–338.
- Scott, R.C., Schuldiner, O., and Neufeld, T.P. (2004). Role and regulation of starvation-induced autophagy in the *Drosophila* fat body. *Dev. Cell* 7, 167–178.
- Simonsen, A., Birkeland, H.C., Gillooly, D.J., Mizushima, N., Kuma, A., Yoshimori, T., Slagsvold, T., Brech, A., and Stenmark, H. (2004). Alfy, a novel FYVE-domain-containing protein associated with protein granules and autophagic membranes. *J. Cell Sci.* 117, 4239–4251.
- Simonsen, A., Cumming, R.C., Lindmo, K., Galaviz, V., Cheng, S., Rusten, T.E., and Finley, K.D. (2007). Genetic modifiers of the *Drosophila* blue cheese gene link defects in lysosomal transport with decreased life span and altered ubiquitinated-protein profiles. *Genetics* 176, 1283–1297.
- Simonsen, A., Cumming, R.C., Brech, A., Isakson, P., Schubert, D.R., and Finley, K.D. (2008). Promoting basal levels of autophagy in the nervous system enhances longevity and oxidant resistance in adult *Drosophila*. *Autophagy* 4, 176–184.
- Steffan, J.S., Bodai, L., Pallos, J., Poelman, M., McCampbell, A., Apostol, B.L., Kazantsev, A., Schmidt, E., Zhu, Y.Z., Greenwald, M., et al. (2001). Histone deacetylase inhibitors arrest polyglutamine-dependent neurodegeneration in *Drosophila*. *Nature* 413, 739–743.
- Strømhaug, P.E., Berg, T.O., Fengsrud, M., and Seglen, P.O. (1998). Purification and characterization of autophagosomes from rat hepatocytes. *Biochem. J.* 335, 217–224.
- Taylor, J.P., Tanaka, F., Robitschek, J., Sandoval, C.M., Taye, A., Markovic-Plese, S., and Fischbeck, K.H. (2003). Aggresomes protect cells by enhancing the degradation of toxic polyglutamine-containing protein. *Hum. Mol. Genet.* 12, 749–757.
- Thurston, T.L., Ryzhakov, G., Bloor, S., von Muhlen, N., and Randow, F. (2009). The TBK1 adaptor and autophagy receptor NDP52 restricts the proliferation of ubiquitin-coated bacteria. *Nat. Immunol.* 10, 1215–1221.
- Vogiatzi, T., Xilouri, M., Vekrellis, K., and Stefanis, L. (2008). Wild type alpha-synuclein is degraded by chaperone-mediated autophagy and macroautophagy in neuronal cells. *J. Biol. Chem.* 283, 23542–23556.
- Wanker, E.E., Scherzinger, E., Heiser, V., Sittler, A., Eickhoff, H., and Lehrach, H. (1999). Membrane filter assay for detection of amyloid-like polyglutamine-containing protein aggregates. *Methods Enzymol.* 309, 375–386.
- Yamamoto, A., Lucas, J.J., and Hen, R. (2000). Reversal of neuropathology and motor dysfunction in a conditional model of Huntington's disease. *Cell* 101, 57–66.
- Yamamoto, A., Cremona, M.L., and Rothman, J.E. (2006). Autophagy-mediated clearance of huntingtin aggregates triggered by the insulin-signaling pathway. *J. Cell Biol.* 172, 719–731.
- Ylä-Anttila, P., Vihinen, H., Jokitalo, E., and Eskelinen, E.L. (2009). 3D tomography reveals connections between the phagophore and endoplasmic reticulum. *Autophagy* 5, 1180–1185.
- Zu, T., Duvick, L.A., Kaytor, M.D., Berlinger, M.S., Zoghbi, H.Y., Clark, H.B., and Orr, H.T. (2004). Recovery from polyglutamine-induced neurodegeneration in conditional SCA1 transgenic mice. *J. Neurosci.* 24, 8853–8861.